ORIGINAL SCIENTIFIC PAPER

CROATICA CHEMICA ACTA

Croat. Chem. Acta **2026**, *99*(1)
Published online: January 17, 2026
DOI: 10.5562/cca4201

HKD 1926

PLA Degrading Enzymes from Metagenomic Databases

Mario Oraić, Dino Koranić, Lucija Brtan, Ivana Kekez,* Aleksandra Maršavelski#

Department of Chemistry, Faculty of Science, University of Zagreb, Horvatovac 102a, 10000 Zagreb, Croatia

* Corresponding author's e-mail address: ikekez@chem.pmf.hr

Corresponding author's e-mail address: amarsavelski.chem@pmf.hr

RECEIVED: August 29, 2025 ✶ REVISED: December 01, 2025 ✶ ACCEPTED: December 11, 2025

PROCEEDING OF THE SOLUTIONS IN CHEMISTRY 2024, 11–15 NOVEMBER 2024, SVETI MARTIN NA MURI, CROATIA

Abstract: In this study, we report the discovery and characterization of novel polylactic acid (PLA)-degrading enzymes sourced from the MGnify metagenomic database. Six candidate enzymes were initially identified, with subsequent efforts focused on two metagenomic enzymes that exhibited better activity and stability compared to the others. A biochemical characterization combined with *N*-terminal modifications was performed to assess the impact of *N*-terminal length and composition on enzyme activity and solubility. Our results underscore the significant potential of metagenomic resources for uncovering new biocatalysts, while also highlighting the critical role of protein engineering in addressing limitations such as low solubility, poor thermostability, and suboptimal expression in heterologous hosts. This work advances the development of efficient biocatalysts for the sustainable degradation and recycling of PLA.

Keywords: polylactic acid, enzyme degradation, esterase, metagenomic database.

INTRODUCTION

POLYLACTIC acid (PLA) is one of the most widely used biodegradable polymers and is frequently promoted as an environmentally friendly alternative to conventional petroleum-based plastics.[1] PLA is synthesized from renewable resources - most notably corn starch, sugarcane, or cassava - via microbial fermentation of carbohydrates into lactic acid, followed by ring-opening polymerization of lactide monomers.[2] As a result of its plant-based origin and theoretically compostable properties, PLA is commonly used in packaging, disposable tableware, textiles, 3D printing, medical devices, and agricultural films.[3] However, despite these perceived ecological advantages, the actual environmental degradation of PLA is often limited under ambient conditions, particularly in soil, freshwater, and home composting systems.[4] Efficient biodegradation of PLA generally requires industrial composting conditions, including elevated temperatures (> 60 °C), controlled humidity, and microbial inoculation to activate the degradation process.[4,5] Outside such controlled environments, PLA can persist for extended periods, leading to accumulation in landfills and natural ecosystems, where its degradation rate is equivalent to or only marginally faster than that of conventional plastics.[6] This discrepancy between theoretical biodegradability and real-world persistence raises critical concerns about PLA's overall environmental impact, especially as its production and usage continue to grow. This resistance is attributed to PLA's high crystallinity and glass transition temperature, which impede microbial and enzymatic attack – highly crystalline PLA shows pronounced resistance to enzymatic hydrolysis beyond a critical crystallinity threshold.[7] Even when known depolymerases are applied, PLA breakdown tends to be surface-limited and can stall as hydrolysis products accumulate; for instance, the release of lactic acid lowers local pH and progressively inactivates the enzymes, slowing further depolymerization. Many of the currently identified PLA-degrading enzymes also exhibit narrow substrate specificity or suboptimal performance. For example, proteinase K (a benchmark PLA-hydrolyzing protease) efficiently depolymerizes poly-L-lactide but

cannot cleave the D-lactide enantiomer (PDLA) due to its stereoselectivity.[8] Likewise, most enzymes favor amorphous regions of PLA, leaving crystalline domains intact unless high temperatures (≥ 60 °C) are employed to increase polymer chain mobility.[7] These limitations underscore the need for new or engineered PLA-depolymerases with greater efficiency, broader specificity, and enhanced stability, motivating the exploration of novel PLA-degrading enzymes (e.g., via metagenomic discovery) to improve sustainable PLA waste management. Currently, PLA dominates the global bioplastics market, accounting for a significant share (37.1 %) of the 2.4 million tonnes of bioplastics produced in 2024.[9] Given its widespread use and contribution to plastic waste streams, there is an urgent need to improve the end-of-life management of PLA. One promising approach is the enzymatic degradation of PLA using microbial hydrolases, which offers a selective, energy-efficient, and environmentally friendly alternative to conventional recycling methods such as thermal degradation, chemical degradation, or incineration.[10] A range of enzymes—including lipases, cutinases, esterases, and proteases—have been shown to hydrolyze the ester bonds in PLA, albeit with variable efficiency and operating conditions.[8,11–12] Some enzymes with polyesterase activity, such as *Ideonella sakaiensis* PETase or *Thermobifida fusca* cutinase, have become model systems for studying synthetic polymer degradation.[13,14] Nevertheless, most of the enzymes currently known to degrade PLA show limitations, including low stability at elevated temperatures, poor performance on semicrystalline polymers, or low expression in microbial hosts commonly used for heterologous production.[15] In recent years, metagenomics has emerged as a powerful approach for discovering novel enzymes from uncultured microbial communities in diverse environments. By circumventing the need for laboratory cultivation, metagenomics enables the direct extraction and cloning of DNA from environmental samples (e.g., soil, marine sediments, geothermal springs, or even spacecraft swabs), vastly expanding the accessible enzymatic diversity.[16] Among the available resources, the MGnify platform, which currently hosts over 2.4 billion non-redundant protein sequences derived from microbiome samples worldwide, has become one of the most comprehensive tools for large-scale biocatalyst discovery.[17] Despite the wealth of sequence data generated by shotgun metagenomics, several major challenges limit the transformation of hypothetical proteins into functional, application-ready enzymes. These include poor solubility, low expression levels, misfolding in *Escherichia coli*, or lack of measurable activity, particularly under industrial or non-native conditions.[18] Moreover, native, wild-type enzymes are often thermally unstable or inefficient when operating on synthetic polymers like PLA.[19] Therefore, protein engineering – whether rational, semi-rational, or through directed evolution – is essential to enhance key features such as thermostability, catalytic efficiency, substrate binding, and resistance to denaturation.[20] In this study, we report the identification, expression, and preliminary sequence manipulation of a set of novel PLA-degrading enzymes sourced from the MGnify metagenomic database. Out of six initially selected candidates, two enzymes were prioritized based on experimental characterization and exhibited promising PLA-degrading activity. One enzyme was evaluated in a truncated form, in its native version, and with *N*-terminal sequence modification, to assess the influence of *N*-terminal length and composition on expression yield, solubility, and activity. Our findings not only highlight the potential of metagenomic approaches to identify untapped biocatalysts for bioplastic degradation but also emphasize the importance of protein engineering in making these enzymes viable for industrial biotechnological applications, particularly those aimed at addressing plastic waste and promoting a circular bioeconomy.

EXPERIMENTAL

Chemicals and Materials

All chemicals were of analytical grade and used without further purification. Luria–Bertani (LB) medium, kanamycin sulfate, sodium chloride, potassium chloride, magnesium chloride, tris(hydroxymethyl)aminomethane hydrochloride (Tris-HCl), 4-(2-hydroxyethyl)piperazine-1-ethanesulfonic acid (Hepes), dl-dithiothreitol (DTT), imidazole, glycerol, dichloromethane, agarose, ethylenedinitrilotetraacetic acid (EDTA), polylactic acid (PLA, average M_w ≈ 100,000) and isopropyl-β-D-thiogalactopyranoside (IPTG) were obtained from Sigma-Aldrich (Merck). Nickel-nitrilotriacetic acid (Ni-NTA) agarose resin was purchased from Qiagen (Hilden, Germany). Plasmids containing synthetic genes were synthesized by Twist Bioscience (San Francisco, CA, USA), *Escherichia coli* BL21(DE3) cells were obtained from Novagen (Merck), and DNase I from Roche (Merck). Superdex 200 Increase 10 / 300 GL column was purchased from Cytiva. A gel-filtration standard mixture containing thyroglobulin, *g*-globulin, ovalbumin, myoglobin, and vitamin B12 was obtained from Bio-Rad. All buffers and solutions were prepared using ultrapure water (18 MΩ cm), which was generated in-house using a Milli-Q system.

Enzyme Selection and Screening

Six enzyme candidates (**A1, A2, A4, 6–3, 6–5,** and **6–6**) were selected from the MGnify metagenomic database (Figure S1) based on sequence homology to two known

PLA-degrading polyesterases. (a) MGS0156 (UniProt ID: A0A0G3FEJ8; PDB ID: 5D8M) – a structurally and biochemically validated polyesterase wth PLA-degrading activity. [21] (b) An MGY polyesterase – an enzyme identified in our laboratory and experimentally characterized to exhibit high hydrolytic activity toward polylactic acid (PLA). Although this enzyme has not yet been published, its catalytic properties and substrate specificity have been confirmed through our internal biochemical assays. In addition, two variants of truncated enzyme **A2** (**A2** lacks its native *N*-terminal sequence) were further tested (FASTA sequences are provided in Figure S1): **A2WS**, which carries its native *N*-terminal sequence; and **A2119N**, a variant containing a 15-amino acid *N*-terminal extension derived from a previously designed enzyme in our laboratory (unpublished results). These variants were included to evaluate how the presence or absence of an *N*-terminal segment, as well as variations in its composition, influence enzyme activity, and solubility. We further hypothesized that the flexibility and unstructured nature of the *N*-terminal region may contribute to polymer–surface interactions, thereby affecting enzyme attachment to polymer and overall activity.

Protein Expression and Purification

Synthetic genes corresponding to six mined sequences (**A1, A2, A4, 6–3, 6–5, 6–6**) and two additional variants (**A2WS, A2119N**) were codon-optimized for *E. coli* expression and cloned into pET-28(a)+ plasmids conferring kanamycin resistance (Twist Bioscience). The constructs were transformed into *E. coli* BL21(DE3) cells by electroporation, and transformants were maintained on LB agar plates containing kanamycin (30 μg mL^{-1}). Glycerol stocks (*v* / *v* 25 %) were prepared and stored at −80 °C. Enzyme variants were expressed in *E. coli* BL21(DE3) using standard molecular biology techniques. Protein expression was optimized at two temperatures (15 °C and 28 °C) to evaluate the effect of temperature on soluble protein yield.[22] Overnight cultures were grown at 37 °C and 250 rpm. For expression at 15 °C, cultures were diluted 1 : 10 into LB medium with kanamycin (30 μg mL^{-1}), using 80 mL for small-scale screening or 1 L for large-scale production. For expression at 28 °C, cultures were diluted 1 : 100 into the same medium. In both cases, cells were grown until an OD_{600} of 0.4–0.6 was reached. Expression was induced with 500 μM IPTG and continued overnight at 15 °C or for 4–5 h at 28 °C. Cells were harvested by centrifugation (5000 g, 15 min, 4 °C), washed, and resuspended in lysis buffer (25 mM Tris-HCl, 500 mM NaCl, (*v* / *v* 10 %*)* glycerol, 1 mM DTT, 10 mM imidazole, 10 μg mL^{-1} DNase I, 4 mM $MgCl_2$). Cells were disrupted by sonication on ice (8 min, 30 s on / off cycles), and cell debris was removed by centrifugation (17000 g, 45 min, 4 °C).

A2, **A2WS**, **A2119N** and **6–5** proteins were purified by Ni-NTA affinity chromatography (Figures S9–S12), and the purity of **A2**, **A2WS**, and **6–5** was further assessed by size-exclusion chromatography (SEC). SEC was performed on a Superdex 200 10 / 300 GL column using an ÄKTA Pure system. Proteins were concentrated with Amicon Ultra centrifugal filters (30 kDa molecular weight cutoff) after Ni–NTA purification and applied to the column in buffer containing 20 mM HEPES-NaOH (pH 7.5), 250 mM NaCl, and 1 mM DTT. For estimation of the oligomerization state, molecular weight standards (thyroglobulin, *g*-globulin, ovalbumin, myoglobin, and vitamin B12) were analyzed on the same column under identical conditions. After each purification step, protein quality was evaluated by SDS-PAGE electrophoresis. Protein concentrations were determined spectrophotometrically at 280 nm using a NanoDrop instrument, with extinction coefficients and molecular masses calculated by the ProtParam program (Table 1).

Table 1. Theoretical molecular masses and molar extinction coefficients of the studied proteins, as calculated using the ProtParam program.

Enzyme	Molecular mass / Da	Molar extinction coefficient / M^{-1} cm^{-1}
A1	37533.36	35870
A2	38704.78	31860
A4	38217.47	30370
6–3	38949.13	31860
6–5	38190.40	30370
6–6	38149.52	34380
A2WS	40474.90	31860
A2119N	40319.61	33350

PLA-Degrading Activity Assay

Initial screening for PLA–degrading activity was performed using agar–polymer clearance assays which is a qualitative test.[23,24] Cell lysates and purified enzymes obtained after affinity chromatography (150 or 225 μg) were tested for activity on agarose plates containing dispersed PLA, with the MGS0156 enzyme serving as a positive control.[21] A clear halo around the protein spot is indicative of hydrolytic activity and degradation of polylactic acid. For plate preparation, 80 mg of PLA was dissolved in 800 μL dichloromethane (DCM) in a 15 mL Falcon tube (final concentration 4 mg mL^{-1}). After complete dissolution, 800 μL of 1 M HEPES-KOH buffer (pH 7.5), 4 μL of 1 M KCl, and 400 μL of 0.5 M EDTA (pH 8.8) were added sequentially, and the volume was adjusted to 20 mL with ultra-pure water. The suspension was sonicated at 60 W for 10 min to generate a stable emulsion, followed by gentle heating in a water bath

to evaporate DCM. Separately, a 0.8 % (*w* / *v*) agarose solution was prepared by dissolving 0.32 g of agarose in 20 mL of ultrapure water, with heating until boiling to ensure complete dissolution. The hot agarose solution was immediately combined with the PLA suspension, and the mixture was poured into sterile 90 mm Petri dishes. Plates were left partially uncovered in a laminar flow hood for 60 min to solidify and allow residual solvent evaporation, then sealed with stretch film and stored at 4 °C until use.

Thermostability Analysis

Differential scanning calorimetry (DSC) was performed on a Nano DSC instrument (TA Instruments) equipped with 300 µL cells. Measurements were carried out over a temperature range of 20 – 110 °C at a heating rate of 1 °C min^{-1}. Protein monomer fractions collected after SEC (fraction 17 for **A2WS**, Figures S7 and S8; fractions 21–23 for **6–5**, Figures S3 and S4) were concentrated to 1 mg mL^{-1} (**A2WS**) or 0.7 mg mL^{-1} (**6–5**) in gel-filtration buffer (20 mM HEPES-NaOH, pH 7.5; 250 mM NaCl; 1 mM DTT). Buffer-against-buffer scans were used for baseline subtraction. Thermograms were processed and analyzed using NanoAnalyze software (version 3.11.0).

RESULTS AND DISCUSSION

Enzyme Screening and Temperature Optimization of Protein Expression

Enzyme screening and temperature optimization of small-scale protein production (80 mL cultures) were carried out to improve the expression, activity, and stability of the six selected enzymes (**A1**, **A2**, **A4**, **6–3**, **6–5**, and **6–6**, (FASTA sequences are provided in Figure S1). Bioinformatic analysis revealed that newly identified candidates (**A1**, **A2**, **A4**, **6–3**, **6–5**, and **6–6**) share moderate sequence similarity with the previously characterized PLA-degrading enzyme MGS0156 (PDB ID: 5D8M) that used as positive control. Pairwise alignments showed 40–44 % sequence identity and 58–61 % positive substitutions, with only 2–5 % gaps across ~ 324–331 aligned residues. All candidates also possess the canonical catalytic triad composed of Ser, His, and Asp. Together, these features suggest that the enzymes retain key catalytic motifs typical of this esterase-like family while exhibiting sufficient sequence divergence to indicate potentially novel biochemical properties. According to the SDS-PAGE analysis of sonicated samples (Figure 1), all proteins tended to form inclusion bodies at both tested temperatures (15 °C and 28 °C), indicating low solubility of all enzymes. Comparatively, enzymes **A2** and **6–5** appeared less abundant in the pellet fraction than the other analysed enzymes (Figure 1). PLA–agarose plate assays with crude cell lysates for all six enzymes did not show any measurable

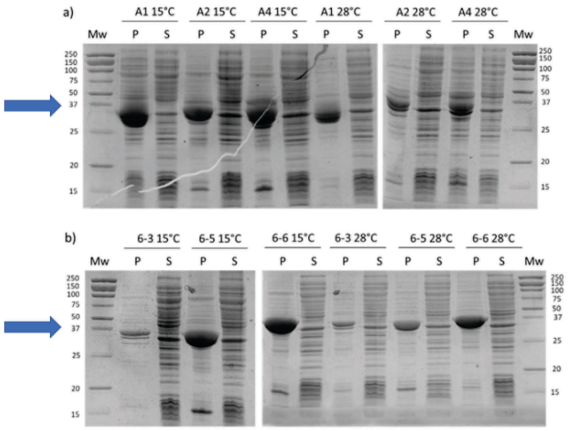

Figure 1. SDS-PAGE analysis of protein fractions after cell lysis (P- pellet; S-supernatant; M_w- molecular weight marker). The culture volume used for protein expression was 80 mL. a) Proteins **A1, A2**, and **A4** obtained from cultures grown at 15 °C (left) and 28 °C (right). b) Proteins **6–3**, **6–5**, and **6–6** from cultures grown at 15 °C (left) and 28 °C (right). The arrow indicates the expected band of the overexpressed proteins. The theoretical molecular masses of the proteins are as follows: **A1**: 37.5 kDa, **A2**: 38.7 kDa, **A4**: 38.2 kDa, **6–3**: 38.9 kDa, **6–5**: 38.2 kDa, **6–6**: 38.1 kDa. Protein bands were visualized using a CCD imaging system.

Table 2. Protein yields from liter-scale cultures after Ni–NTA chromatography. Induction temperatures of the cultures are indicated in the table.

	m (protein) / mg			
t / °C	**6–5**	**A2**	**A2WS**	**A2119N**
15 °C	0.92	4.93	1.03	1.08
28 °C	0.61	2.76	–	–

activity toward PLA (Figure 2a). Based on these results, enzymes **A2** and **6–5** were selected for further evaluation of expression levels on a larger-scale production (1 L culture volume) and for assessment of activity against PLA after Ni-NTA purification (Figures S9 and S12). Enzyme **A2** showed significantly higher expression yield of soluble fractions at 15 °C (*m* = 4.93 mg) compared to 28 °C (*m* = 2.76 mg) as seen in Table 2. This observation is consistent with reports that low-temperature expression reduces aggregation and improves solubility by slowing protein synthesis and facilitating proper folding, thereby minimizing inclusion body formation.[22] In contrast, enzyme **6–5** exhibited lower yields of soluble fractions at both 15 °C (*m* = 0.92 mg) and 28 °C (*m* = 0.61 mg), Table 2.

As the qualitative PLA–agarose plate assays with crude cell lysates did not show measurable activity toward

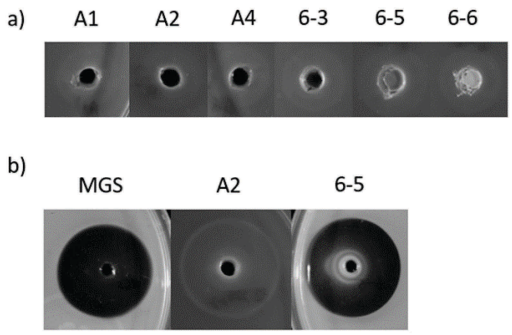

Figure 2. Enzymatic activity was tested qualitatively by using PLA–agarose plates assay. (a) Cell lysates (20 µL) applied. (b) Concentrated protein fractions after Ni–NTA purification: **MGS0156** enzyme[21] (150 µg, positive control, 14 days), **A2** enzyme (225 µg, 31 days), and **6–5** enzyme (150 µg, 14 days).

PLA (Figure 2a), we next tested whether the purified enzymes **A2** and **6–5** display activity (Figure 2b). While the positive control **MGS0156** [21] produced a clear halo within 14 days, enzyme **A2** showed only marginally detectable activity compared to the control, even after prolonged incubation (31 days). In contrast, enzyme **6–5** exhibited strong clearance within 14 days, demonstrating robust PLA-degrading activity. Notably, crude lysates of **6–5** showed no detectable activity. While it is possible that the remaining four enzymes might also show weak activity after purification, their low soluble expression levels and poor overall yields made them less promising candidates for further purification and additional assays for these variants. This discrepancy can be explained by several factors. Crude lysates contain a complex mixture of cellular proteins, metabolites, and potential inhibitors that can mask or interfere with the activity of the target enzymes. In addition, the relatively low abundance of heterologously expressed enzymes in crude extracts may have been insufficient to generate visible hydrolysis zones on the plate. By contrast, purification enriches the enzyme of interest, increasing its effective concentration relative to background proteins and thereby enhancing the likelihood of substrate degradation. Furthermore, purification removes host proteins that might bind nonspecifically to PLA, compete for cofactors, or even destabilize the enzyme, all of which could suppress apparent activity in crude lysates. Finally, agarose plate assays are relatively insensitive and may not detect weak activities in complex mixtures; once purified, the enzyme activity becomes more readily discernible above background. Collectively, these considerations explain why measurable PLA hydrolysis was observed only after purification.

All these findings suggested that among the six initially selected enzymes (**A1**, **A2**, **A4**, **6–3**, **6–5**, and **6–6**), only **A2** and **6–5** showed sufficient solubility and activity to proceed with further sequence and purification optimization. So, the remaining candidates (**A1**, **A4**, **6–3**, and **6–6**) were excluded from subsequent experiments.

Enhancing the Sequence Stability and Activity Through Sequence Engineering

Due to the highest solubility (Table 2), enzyme **A2** was selected for further testing. Because the expressed **A2** construct is truncated at the *N*-terminus, we also tested **A2WS**, carrying its native *N*-terminal sequence, and **A2119N**, a variant with a 15-amino acid *N*-terminal extension derived from a previously engineered enzyme (unpublished results), to assess the impact of *N*-terminal length and composition on surface attachment and subsequent activity (Figure S1). It is known that for polyester hydrolases, *N*-terminal regions have demonstrable effects on structure and activity. In *Ideonella sakaiensis* PETase, deletion of the first seven *N*-terminal residues disrupts the *N*–*C* terminal hydrogen-bonding network, reducing thermostability and PET-binding affinity.[25] Likewise, truncation of the *N*-terminal domain in Clostridium botulinum esterase (Cbotu_EstA) substantially improved PET hydrolysis — resulting in exposing a hydrophobic patch on the surface and improved sorption of hydrophobic polyesters, concomitantly facilitating the access of the polymer to the active site.[26] In addition, protein adsorption studies show that *N*-terminal regions frequently mediate the initial surface-contact event. In the rice seed protein Rsn-2, the flexible, hydrophobic *N* terminus docks onto the oil–water interface first. Deletion mutants lacking *N*-terminal residues (ΔL1–L3 and ΔL1–P15) exhibit greatly reduced adsorption rates, demonstrating that the *N*-terminus recruits the protein to interfaces.[27] Similarly, a textbook enzyme lysozyme adsorbs to charged surfaces and its natural polymeric substrate peptidoglycan via its *N*/*C*-terminal face; Arg128 is a key anchoring residue that mediates electrostatic interaction with negatively charged interfaces, followed by residues Lys1 and Arg5.[28]

Both variants, **A2WS** and **A2119N**, were successfully expressed at 15 °C but in lower yields (*m* ≈1 mg) compared to the truncated **A2** enzyme, Table 2, and tested against PLA activity after Ni-NTA chromatography (Figures S10 and S11). As evident from PLA–agarose plate assays (Figures 2b and 3), the intact variant **A2WS** exhibited detectable activity against PLA, comparable to truncated **A2**. In contrast, the **A2119N** variant produced only a faint halo, indicating much lower activity. These results highlight the delicate balance in protein sequence manipulation and engineering, where modifications introduced to improve activity can also reduce solubility and vice versa.

Stability Studies of A2, A2WS and 6–5

To investigate soluble aggregate formation and oligomerization state, size-exclusion chromatography (SEC) was performed for **A2**, **A2WS**, and **6–5** expressed at 15 °C. All three enzymes displayed a predominant peak corresponding to the monomeric form (Figures 4 and 5), as determined by comparison of elution volumes with molecular weight standards (Table S1, Figures S2–S8). These results indicate proper folding and the absence of significant aggregation.

To further assess enzyme stability, differential scanning calorimetry (DSC) was performed on the most active PLA-degrading enzymes (**A2WS** and **6–5**). DSC analyses revealed distinct melting temperatures: **A2WS** (t_m = 42.94 °C) and **6–5** (t_m = 55.21 °C) (Figure 6). Compared to **A2WS**, enzyme **6–5** demonstrated both higher thermostability and stronger PLA-degrading activity, although expression levels remained similarly low for both. Thus, **6–5** emerges as the more promising candidate; however, further sequence optimization will be necessary to enhance expression and stability for potential application in industrial polymer degradation.

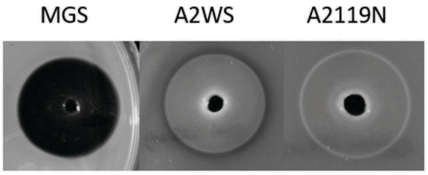

Figure 3. Enzymatic activity was tested qualitatively by using PLA–agarose plates assay. Concentrated protein fractions after Ni-NTA purification: **MGS0156** enzyme[21] (150 µg, positive control, 14 days), **A2WS** enzyme (225 µg, 31 days), and **A2119N** enzyme (150 µg, 31 days).

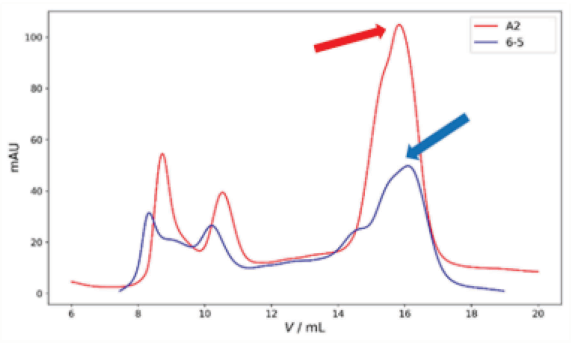

Figure 4. Size-exclusion chromatography (SEC) profiles of enzymes **A2** (blue) and **6–5** (red) expressed at 15 °C. The arrows indicate the monomeric form of the protein. The theoretical molecular masses of the proteins are as follows: **A2**: 38.7 kDa, **6–5**: 38.2 kDa.

Modeling

Enzymes **A2** and **6–5** were modeled using the AlphaFold3 to gain insights into their three-dimensional conformation.[29] Structural analysis of the AlphaFold-predicted models enabled the identification of a conserved catalytic triad, characteristic of polyesterases, which is likely essential for PLA polymer degradation. Sequences

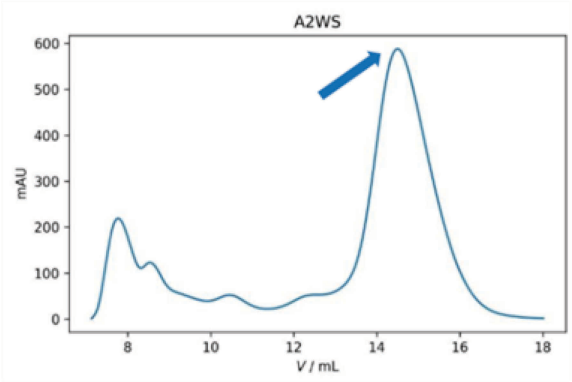

Figure 5. Size-exclusion chromatography (SEC) profile of enzyme **A2WS**. The arrow indicates the monomeric form of the protein. The theoretical molecular mass of enzyme **A2WS** is 40.5 kDa.

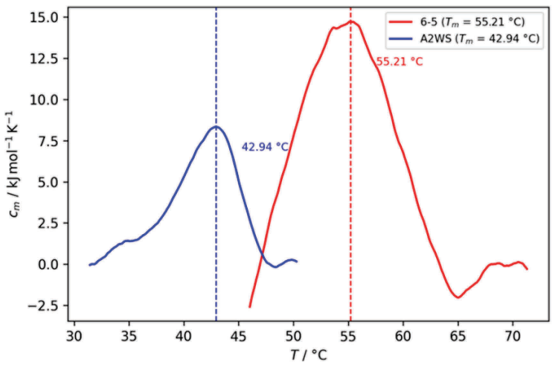

Figure 6. Thermal denaturation profiles (thermograms) of enzymes **A2WS** (blue) and **6–5** (red).

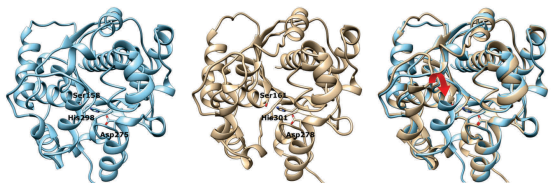

Figure 7. Predicted structures of enzyme **A2** (cyan) and enzyme **6–5** (tan), with their catalytic triads highlighted. The superimposed structures reveal the characteristic α/β-hydrolase fold. The red arrow indicates the closed lid conformation observed in **A2** compared to the more open lid in **6–5**.

that we have used for modelling are those that correspond to expressed protein including His_6-tag, followed by a TEV protease cleavage site (Figure S1). According to the AlphaFold model, the predicted catalytic triad of enzyme **A2** is Ser158, Asp275 and His298 and for **6–5** enzyme is Ser161, Asp278 and His301 (Figure 7).

CONCLUSION

This study highlights several key challenges in metagenomic enzyme discovery and development. A major limitation is that most metagenomic sequences are uncharacterized and not optimized for expression in heterologous hosts such as *E. coli*. Differences in codon usage, protein folding pathways, and cellular environments between native microbial sources and laboratory hosts contribute to poor expression outcomes.

Low solubility was observed for most enzyme candidates, reflecting a common bottleneck in heterologous expression, where proteins misfold and aggregate into inclusion bodies. This challenge is particularly pronounced for enzymes from environmental microorganisms that evolved under conditions markedly different from those in laboratory systems. Among the six enzymes tested, only two, **6–5** and **A2WS**, showed significant and detectable activity, respectively, underscoring both the difficulty of functional discovery and the necessity of enzyme property optimization. Overall, the contrasting behaviors of the truncated **A2** and the longer **A2WS** and **A2119N** variants—where both extended forms showed lower yield and solubility, despite **A2WS** with its native *N*-terminus exhibiting only a slight activity increase—underscore how *N*-terminal engineering can produce unpredictable and often counterintuitive effects on enzyme performance.

Despite these challenges, this work demonstrates the potential of metagenomic mining for identifying novel PLA-degrading enzymes. Resources such as MGnify provide access to vast enzymatic diversity, but converting this diversity into functional biocatalysts requires systematic protein engineering. The successful identification of enzyme **A2**, together with the characterization of enzyme **6–5**, establishes a foundation for further development. The key takeaways from this study are: (1) metagenomic databases are valuable sources of novel enzymatic activities; (2) solubility remains a critical barrier in enzyme development from metagenomic sources; and (3) newly discovered enzymes require extensive optimization—through protein engineering to enhance solubility, tune activity and selectivity, and improve thermostability—to unlock their potential for industrial applications.

Acknowledgment. M.O. and D.K. acknowledge the Young Researcher and Innovator Conference grants from COST Action CA21162. A.M. acknowledges the Development Research Support funded through National Recovery and Resilience Plan (NextGenerationEU) for the project Enzyme Engineering for sustainable recycling of bioplastics (NPOO.C3.2.R2-I1.06.0041)

Supplementary Information. Supporting information to the paper is attached to the electronic version of the article at: https://doi.org/10.5562/cca4201.

PDF files with attached documents are best viewed with Adobe Acrobat Reader which is free and can be downloaded from Adobe's web site.

REFERENCES

[1] M. Jamshidian, E. A. Tehrany, M. Imran, M. Jacquet, S. Desobry, *Compr. Rev. Food. Sci.* **2010**, *9*, 552–571. https://doi.org/10.1111/j.1541-4337.2010.00126.x

[2] W. Ali, H. Ali, S. Gillani, P. Zinck, S. Souissi, *Environ. Chem. Lett.* **2023**, *21*, 1761–1786 https://doi.org/10.1007/s10311-023-01564-8

[3] T. D. Moshood, G. Nawanir, F. Mahmud, F. Mohamad, M. H. Ahmad, A. AbdulGhani, *Curr. Res. Green Sustain. Chem.* **2022**, *5*, 100273-100281. https://doi.org/10.1016/j.crgsc.2022.100273

[4] S. V. Afshar, Alessio Boldrin, T. F. Astrup, A. E. Daugaard, N. B. Hartmann, *J. Clean. Prod.* **2024**, *434*, 140000–140024 https://doi.org/10.1016/j.jclepro.2023.140000

[5] M. Hussain, S. M. Khan, M. Shafiq, N. Abbas, *Giant* **2024**, *18*, 100261-100292 https://doi.org/10.1016/j.giant.2024.100261

[6] T. P. Haider, C. Völker, J. Kramm, K. Landfester, F. R. Wurm, *Angew. Chem. Int. Ed.* **2018**, *58*, 50–62. https://doi.org/10.1002/anie.201805766

[7] A. Pustak, A. Maršavelski, *FEBS Open Bio* **2025**, https://doi.org/10.1002/2211-5463.70177

[8] A. Shalem, O. Yehezkeli, A. Fishman, *Appl. Microbiol. Biotechnol.* **2024,** *108*, 413 https://doi.org/10.1007/s00253-024-13212-4

[9] European Bioplastics, Bioplastics market development update 2024, https://www.european-bioplastics.org/market/

[10] Y. Tokiwa, B. P. Calabia, Appl. Microbiol. Biotechnol. **2006**, *72*, 244–251. https://doi.org/10.1007/s00253-006-0488-1

[11] W. Zhang, C Li, H. Liang, Z. Wang, *Int. J. Biol. Macromol*. **2025**, *314*, 144410 https://doi.org/10.1016/j.ijbiomac.2025.144410

[12] G. Sourkouni, S. Jeremić, C. Kalogirou, O. Höfft, M. Nenadovic, V. Jankovic, D. Rajasekaran, P. Pandis, R. Padamati, J. Nikodinovic-Runic, C. Argirusis, *World J. Microbiol. Biotechnol.* **2023,** *39*, 161 https://doi.org/10.1007/s11274-023-03605-4

[13] S. Yoshida, K. Hiraga, T. Takehana, I. Taniguchi, H. Yamaji, Y. Maeda, K. Toyohara, K. Miyamoto, Y. Kimura, K. Oda, *Science* **2016**, *351,* 1196–1199. https://doi.org/10.1126/science.aad6359

[14] R.-J. Müller, H. Schrader, J. Profe, K. Dresler, W.-D. Deckwer, *Macromol. Rapid Commun.* **2025**, *26*, 1400-1405 https://doi.org/10.1002/marc.200500410

[15] F. Rahmati, D. Sethi, W. Shu, B. A. Lajayer, M. Mosaferi, A. Thomson, and G. W. Price, *Chemosphere* **2024**, *355*, 141749 https://doi.org/10.1016/j.chemosphere.2024.141749

[16] J. Handelsman, *Microbiol. Mol. Biol. Rev.* **2004**, *68*, 669–685. https://doi.org/10.1128/MMBR.68.4.669-685.2004

[17] L. Richardson, B. Allen, G. Baldi, M. Beracochea, M. L. Bileschi, T. Burdett, J. Burgin, J. Caballero-Pérez, G. Cochrane, L. J. Colwell, T. Curtis, A. Escobar-Zepeda, T. A. Gurbich, V. Kale, A. Korobeynikov, S. Raj, A. B. Rogers, E. Sakharova, S. Sanchez, D. J. Wilkinson, R. D. Finn, *Nucleic. Acids. Res.* **2023**, *51*, D753–D759, https://doi.org/10.1093/nar/gkac1080

[18] M. Pouresmaeil, S. Azizi-Dargahlou, *Arch. Microbiol.* **2023**, *205*, 212 https://doi.org/10.1007/s00203-023-03541-9

[19] RT. Guo, X. Li, Y. Yang, et al. *Environ. Chem. Lett.* **2024**, *22*, 1275–1296. https://doi.org/10.1007/s10311-024-01714-6

[20] B. Zhu, D. Wang, N. Wei, *Trends Biotechnol.* **2022**, 40, 22-37 https://doi.org/10.1016/j.tibtech.2021.02.008

[21] M. Hajighasemi, A. Tchigvintsev, B. Nocek, R. Flick, A. Popovic, T. Hai, A. N. Khusnutdinova, G. Brown, X. Xu, H. Cui, J. Anstett, T. N. Chernikova, T. Brüls, D. Le Paslier, M. M. Yakimov, A. Joachimiak, O. V. Golyshina, A. Savchenko, P. N. Golyshin, E. A. Edwards, A. F. Yakunin, *Environ. Sci. Technol.* **2018**, *52*, 12388–12401. https://doi.org/10.1021/acs.est.8b04252

[22] C. H. Schein, M. H. M. Noteborn, *Nature Biotechnology* **1988**, *6*, 291–294. https://doi.org/10.1038/nbt0388-291

[23] T. Teeraphatpornchai, T. Nakajima-Kambe, Y. Shigeno-Akutsu, M. Nakayama, N. Nomura, T. Nakahara, H. Uchiyama, *Biotechnol. Lett.* **2003**, *25*, 23–28. https://doi.org/10.1023/A:1021713711160

[24] M. Hajighasemi, B. P. Nocek, A. Tchigvintsev, G. Brown, R. Flick, X. Xu, H. Cui, T. Hai, A. Joachimiak, P. N. Golyshin, A. Savchenko, E. A. Edwards, A. F. Yakunin, *Biomacromolecules* **2016**, *17*, 2027–2039. https://doi.org/10.1021/acs.biomac.6b00223

[25] N. G. Nezhad, S. B. Buhari, A. Eskandari, et al., 3 Biotech **2025**, *15*, 93. https://doi.org/10.1007/s13205-025-04258-w

[26] A. Biundo, D. Ribitsch, G. Steinkellner, K. Gruber, G. M. Guebitz, Biotechnology Journal **2016**, *12* 11. https://doi.org/10.1002/biot.201600450

[27] G. B. Brandani, S. J. Vance, M. Schor, A. Cooper, M. W. Kennedy, B. O. Smith, C. E. MacPhee, D. L. Cheung, Phys. Chem. Chem. Phys. **2017**, *19*, 8584–8594. https://doi.org/10.1039/C6CP07261E

[28] K. Kubiak-Ossowska, P. A. Mulheran, Langmuir, **2012**, *28*, 15577–15585. https://doi.org/10.1021/la303323r

[29] J. Abramson, J. Adler, J. Dunger, R. Evans, T. Green, A. Pritzel, O. Ronneberger, L. Willmore, A. J. Ballard, J. Bambrick, S. W. Bodenstein, D. A. Evans, C.-C. Hung, M. O'Neill, D. Reiman, K. Tunyasuvunakool, Z. Wu, A. Žemgulytė, E. Arvaniti, C. Beattie, O. Bertolli, A. Bridgland, A. Cherepanov, M. Congreve, A. I. Cowen-Rivers, A. Cowie, M. Figurnov, F. B. Fuchs, H. Gladman, R. Jain, Y. A. Khan, C. M. R. Low, K. Perlin, A. Potapenko, P. Savy, S. Singh, A. Stecula, A. Thillaisundaram, C. Tong, S. Yakneen, E. D. Zhong, M. Zielinski, A. Žídek, V. Bapst, P. Kohli, M. Jaderberg, D. Hassabis, J. M. Jumper, *Nature* **2024**, *630*, 493–500. https://doi.org/10.1038/s41586-024-07487-w